

Research

Systematically investigate the mechanism underlying the therapeutic effect of emodin in treatment of prostate cancer

Gang Yuan¹ · Jingxin Mao² · Zheng Li³

Received: 22 September 2024 / Accepted: 13 March 2025

Published online: 27 March 2025

© The Author(s) 2025 **OPEN**

Abstract

Objective To systematically investigate the mechanism underlying the therapeutic effect of emodin in treatment of prostate cancer.

Methods Combine network pharmacology, molecular docking, molecular dynamics and experimental verification to explored the mechanism. Using the network pharmacology method, through the TCMSP, DisGeNET and Genecards database, the corresponding targets and related signaling pathways of emodin were screened, and emodin and core targets were studied by molecular docking and molecular dynamics using Cytoscape 3.7.2 and other software. The biological processes, cellular components and molecular functions of the key targets were determined by GO enrichment analysis. KEGG enrichment analysis identified signaling pathways associated with key targets. GEPIA and Kaplan–Meier database were used to determine the relationship between the expression of core genes in normal people and prostate cancer patients and the prognosis of patients. Cell proliferation inhibition experiment was carried out by MTT method. The mRNA and protein levels of CASP3, TNF, IL1B, TP53, PPARG, and MYC in PC-3 cells were evaluated by RT-PCR and WB method respectively.

Results There were 31 common targets which closely related to emodin in the treatment of prostate cancer. PPI network analysis showed that MYC, PPARG, TP53, TNF, CASP3, IL1B were the core targets. Go and KEGG enrichment analysis showed that pathways in cancer and IL-17 signaling pathway were the key pathways. Molecular docking and molecular dynamics results indicated that emodin had good binding to prostate cancer and 6 core proteins, and the binding force with TP53 protein was the strongest and most stable. The expression of CASP3 protein in normal people was stronger than that in patients with prostate cancer, and the expression of TP53 protein was closely related to the survival rate of patients with prostate cancer. Experimental verification result revealed that EM significantly increased mRNA expressions of CASP3, PPARG and decreased protein expressions of TNF, TP53, MYC at concentrations ranging from 0.1 to 1.6 $\mu\text{mol/L}$. Emodin significantly increased protein expressions of CASP3, PPARG and decreased protein expressions of TNF, TP53, MYC, IL1B at concentrations ranging from 10 to 160 $\mu\text{mol/L}$.

Jingxin Mao and Zheng Li contributed equally to this work.

Supplementary Information The online version contains supplementary material available at <https://doi.org/10.1007/s12672-025-02141-x>.

✉ Jingxin Mao, 2230040@cqmpc.edu.cn; maomao1985@email.swu.edu.cn; ✉ Zheng Li, bigrain218@outlook.com | ¹Pharmacy Department, Jiulongpo Hospital of Chongqing University of Chinese Medicine, Chongqing Jiulongpo Traditional Chinese Medicine Hospital, Chongqing 400050, China. ²Chongqing Medical and Pharmaceutical College, No. 82, Middle Road of University Town, Shapingba District, Chongqing 400030, China. ³Pharmacy Department, Chongqing University Affiliated Renji Hospital, No. 121 Wangxi Road, Nan'an District, Chongqing 401336, China.



Conclusion Emodin and TP53 have the best binding and stable conformation among core genes. Emodin exhibits a significant inhibitory effect on PC-3 cells at concentration 0.4 ~ 1.6 $\mu\text{mol/L}$. It showed that anti-prostate cancer properties by regulating cancer and 1L-17 signaling pathway through up-regulating the expressions of CASP3, PPARG genes/proteins, down-regulating IL1B, TP53, TNF, MYC genes/proteins.

Keywords Prostate cancer · Network pharmacology · Molecular docking · Therapeutic effect · Experimental verification · Pharmacological mechanism

1 Introduction

Prostate cancer (PCa) is one of the malignant tumors with a relatively high clinical incidence rate, characterized by strong concealment and poor prognosis. According to the 2019 statistics from the American Cancer Society (ACS), PCa ranks first in male incidence and second in mortality [1]. Recent cancer statistics in China have revealed that with the country's economic growth and changes in lifestyle, work-rest routines, and dietary habits, the incidence of PCa has also shown a rapid upward trend [2]. The etiology of PCa is complex and diverse, and is not fully elucidated yet. However, age, ethnicity, and family history of the disease are recognized as risk factors [3]. PCa is relatively rare in young men and below, while its incidence and mortality rates significantly increase in middle-aged and elderly men, with both incidence and aggressiveness rising with age [4]. Statistics from the ACS show that African Americans have the highest rate of PCa, with an incidence rate nearly 60% higher and a mortality rate more than twice as high compared to European Americans [5, 6]. There is a close causal relationship between genetic factors and the occurrence of PCa. Individuals with a genetic link to someone diagnosed with PCa have a 2 ~ 3 times higher risk of developing prostate malignancy than those without a family history of PCa [7].

Currently, the main treatments for PCa mainly including surgery, radiotherapy, chemotherapy, and endocrine therapy. Clinically, appropriate treatment methods are selected based on the patient's actual condition, and a combination of multiple treatment methods may be adopted when necessary. Radical prostatectomy and radiotherapy are the primary treatments for early-stage PCa [8, 9]. It has been reported that radical prostatectomy exhibits excellent efficacy in localized early-stage PCa, reducing cancer-specific mortality among men with localized PCa. However, it was reported that postoperative prostate-specific antigen (PSA) levels may increase in some patients, with a recurrence rate as 30% [10, 11].

The symptoms of early PCa are not obvious and difficult to detect. Most patients are already in the middle or advanced stage when they are diagnosed, losing the opportunity for radical surgery and radiotherapy. At this point, androgen deprivation therapy (ADT) becomes the primary treatment method. However, after 18 to 36 months of treatment, almost all patients will develop into castration-resistant prostate cancer (CRPC). Consequently, the clinical treatment outcomes for CRPC patients are poor, with extremely poor prognosis and short median survival time [12]. Additionally, chemotherapeutic drugs such as docetaxel, while effective in treating the disease, also cause a series of side effects including bone marrow suppression, gastrointestinal reactions, and impaired immune function [13]. With the advancement of medicine, the diversified comprehensive treatment of PCa has become increasingly sophisticated. Traditional Chinese medicine (TCM), as an important auxiliary and complementary therapy, has demonstrated proven efficacy and has been widely applied [14].

Emodin (EM) is an anthraquinone compound and one of the active ingredients found in *Polygonaceae* plants such as *Rheum palmatum*, *Rheum tanguticum*, or *Rheum officinale*. Its molecular formula is $\text{C}_{15}\text{H}_{10}\text{O}_5$, and its chemical name is 1,3,8-trihydroxy-6-methylantraquinone [15]. Previous research has demonstrated that EM possesses various anti-tumor biological effects. Specifically, EM at concentrations ranging from 10 to 80 $\mu\text{mol/L}$ can significantly reduce the viability of colon cancer cells, inducing cell cycle arrest and apoptosis in these cells [16]. At concentrations between 25 and 100 $\mu\text{mol/L}$, EM inhibits the proliferation of MCF-7 human breast cancer cells [17]. Furthermore, 30 $\mu\text{mol/L}$ of EM can suppress the proliferation of non-small cell lung cancer cells by regulating the cell cycle [18]. Additionally, EM can induce apoptosis in tumor cells by influencing the expression of cysteinyl aspartate specific proteinase (casp) 3 and casp 9, thereby playing a therapeutic role in pancreatic cancer [19]. Nuclear factor- κB (NF- κB) and signal transducer and activator of transcription (STAT) have emerged as key regulators of cancer-related inflammation. EM at 15 $\mu\text{mol/L}$, after 48 h of treatment, can modulate the expression and localization of B-cell lymphoma 2 (bcl-2) family proteins in human colon cancer COLO201 cells by regulating molecular signaling pathways such as I κB kinase β (IKK β)/NF- κB and signal transducer and activator of transcription (STAT), thereby regulating tumor cell proliferation, differentiation, and apoptosis [14]. In vivo experiments have shown that EM inhibits the secretion of secretory small

molecular phospholipase A2-IIa (sPLA2-IIa) in C57 mice, which subsequently inhibits NF- κ B activity, leading to the death of non-small cell lung cancer cells [20].

Meanwhile, it was revealed that EM may enhance the cytotoxicity of chemotherapeutic drugs on PCa cells. The mechanism involves reactive oxygen species (ROS) mediated inhibition of multidrug resistance and the expression level of hypoxia inducible factor (HIF) -1 in recent years [21]. In addition, EM was proved to directly target androgen receptor (AR) to inhibit the growth of PCa cells in vitro, reduce the binding of AR and heat shock protein 90 (HSP90), and increase the binding of AR and murine double minute 2 (MDM2), thus inducing AR degradation through proteasome mediated pathway in a ligand independent manner, and prolonging the survival time of C3 (1) /simian virus 40 transgenic mice in vivo [22].

The vast majority of existing treatment modalities fail to eradicate PCa, often resulting in significant toxicity and adverse effects. Consequently, the pursuit of more efficacious therapeutic agents has emerged as a pressing research focus and challenge. It was reported that EM exhibit varies biological activities and functions mainly including anti-inflammatory [23], anti-tumor [24], immune regulation [25] and others. It may treat urinary system diseases in clinic, and has good therapeutic effect on prostatitis [26]. However, the mechanism of EM against PCa is not deep enough, and more in-depth research is urgently needed. Network pharmacology is an interdisciplinary combining multidirectional pharmacology, molecular network data, bioinformatics and computer simulation, which has been widely used by researchers of TCM [27]. In recent years, with the mature application of molecular detection technology and the continuous discovery of signal pathways and pathogenic genes in tumor tissues, the treatment of PCa has gradually become more precise, and the targeted treatment for signal pathway transmission is more mature. Therefore, the present study used the method of network pharmacology combining molecular docking and molecular dynamics to explore the potential therapeutic effect and mechanism of EM on PCa and provide further theoretical reference for clinical treatment.

2 Materials and methods

All of the database and software which used in the present study were presented in Table 1. The details of materials and methods as following:

Table 1 Database and software which used in the study

Name of Database and software	Website address
TCMSP Database	https://www.tcmsp-e.com/#/database/
DisGeNET Database	https://www.disgenet.org/
UniProt Database	https://www.uniprot.org/
Genecards Database	https://www.genecards.org/
Venny 2.1 Online Software	https://bioinfogp.cnb.csic.es/tools/venny/index.html/
STRING 11.1 Online Database	https://string-db.org/
DAVID 6.8 Database	https://david.ncifcrf.gov/
LC-BIO Online Analysis Platform	https://www.omicstudio.cn/
GEPIA Online Database	http://gepia2.cancer-pku.cn/
Kaplan–Meier Plotter Online Database	http://kmplot.com/analysis/
PubChem Database	https://pubchem.ncbi.nlm.nih.gov/
PDB Database	https://www.rcsb.org/
Cytoscape 3.7.2 Software	http://cytoscape.org/
Pymol 2.4.0 Software	https://www.pymol.org/
OpenBabel 2.4.1	https://pypi.org/project/openbabel/2.4.1/
Perl 5.24.1 Software	https://dev.perl.org/perl5/news/2017/perl-5.24.1.html
GraphPad Prism 9 Software	https://www.graphpad.com/
R 4.0.5 Software	https://www.r-project.org/
Discovery Studio 2019 Software	https://www.3ds.com/products/biovia/discovery-studio/

2.1 Acquisition of EM

The EM (CAS number: 518-82-1) was obtained from Wuhan Kabuda Chemical Co., Ltd with a purity of 99%. Its molecular formula is $C_{15}H_{10}O_5$, molecular weight is 270.23, melting point is between 256 °C and 257 °C.

2.2 Acquisition of EM molecular targets

All target information of EM was retrieved through Traditional Chinese Medicine Systems Pharmacology Database and Analysis Platform (TCMSP) database. The target of EM was found by Perl 5.24.1 software, and the gene names of EM target were annotated by UniProt database.

2.3 Screening the target interactions of “EM and PCa”

Using “tumor” and “cancer” as keywords, the target genes of PCa were screened by Genecards database and DisGeNET database, and the disease correlation score ≥ 1 as the reference value. Finally, utilization of R 4.0.5 software and Venny 2.1 online software, the EM target genes and PCa target genes were intersected to obtain their common target genes.

2.4 Construction of “compound-disease-target” network between EM and PCa

The common target genes screened by the above process were imported into Cytoscape 3.7.2 software to construct “EM-PCa target” network.

2.5 Protein/gene-protein/gene interaction (PPI) network analysis

Protein/gene-protein/gene interaction (PPI) network was made through the string database, and the intersection was evaluated with the plug-in “cytonca” to obtain the protein–protein interaction network core. Cytonca uses three centrality measures for data selection, which including degree centrality (DC), closeness centrality (CC), and betweenness centrality (BC). Firstly, the database is selected according to the standard of “DC ≥ 2 times the median”, and then the core target is selected according to the standard of “DC, BC, and CC \geq the median” [6].

2.6 Gene Ontology (GO) analysis and Kyoto Encyclopedia of genes and genomes (KEGG) pathway analysis

R 4.0.5 software and LC-BIO online analysis platform were used to perform GO enrichment analysis and KEGG analysis on the targets of EM regulating PCa. “Homo sapiens” was used as the limited species, so as to obtain the results of GO enrichment analysis and KEGG pathway enrichment analysis.

2.7 Molecular docking and visualization of docking results

Download the 3D structure of emodin through PubChem database, take the core target obtained by “cytonca” plug-in as the receptor protein, find its accurate protein name through UniProt database, and then download the 3D structure of the core target molecule through PDB database. Import pymol 2.4.0 software for dehydration, ligand removal, hydrogenation and other treatments, and minimize the energy of the docking target. Then, the core gene was processed into mol2 format with the help of openbabel 2.4.1 software, and then the molecular docking between EM and the core targets were carried out with the help of Discovery Studio 2019 software. The lower the energy of molecular docking, the more stable the conformation of receptor molecule in docking. Finally, openbabel 2.4.1 and pymol 2.4.0 software were used for visual analysis of docking results.

2.8 Molecular dynamics simulation

The “CHARMM” and “simulation protocols” modules of Discovery Studio 2019 software were used to add charmm36 force field to the “TP53/EM” molecular structure model constructed by precise docking, and then the model was solvated,

that is, the model was placed in a $110 \text{ \AA} \times 110 \text{ \AA} \times 110 \text{ \AA}$ aqueous solution cubic box. The molecular dynamics simulation parameters are set as follows: the temperature increases gradually from 50 to 300 K, and the simulation time is 220 PS, including 20 ps in the equilibrium phase and 2 ns in the simulation sampling phase.

2.9 Expression of key genes and survival prognosis analysis

The gene expression profiling interactive analysis (GEPIA) is a multidimensional cancer genomics dataset that integrates a large amount of data from the Cancer Genome Atlas (TCGA) and the genotype tissue expression project (GTEx). GEPIA database was used to screen the expression differences between normal prostate cancer tissues and PCa tissues. The parameters were set as default, and $P < 0.05$ was considered statistically significant. According to the expression levels of 6 core genes, PCa samples were divided into two groups (low expression group and high expression group). Kaplan Meier-plotter online database can be used to evaluate the prognostic impact of different genes on different cancers. Overall survival (OS) was considered as the time to death or the last follow-up time since the initial diagnosis of PCa.

2.10 Cell level experimental verification

2.10.1 Cell lines and culture

The PC-3 cells were acquired from the Stem Cell Bank of the Chinese Academy of Sciences. As a culture medium, Dulbecco's Modified Eagle Medium (DMEM) supplemented with 10% Fetal Bovine Serum (FBS) and a combination of antibiotics, specifically 100 U/mL of penicillin and 100 $\mu\text{g/mL}$ of streptomycin, was employed respectively. The cells were then maintained in an incubator set at 37°C and 5% CO_2 concentration.

2.10.2 Cell proliferation and inhibition experiment

Inoculate PC-3 cells at a density of 1×10^4 cells/mL into a 96 well culture plate, with 190 μL per well. Incubate overnight in a constant temperature saturated incubator containing 5% CO_2 at 37°C and divide into two groups: the experimental group is treated with 10 μL of different concentrations (0.1 ~ 1.6 $\mu\text{mol/L}$) of emodin, while the control group (Con) is treated with 10 μL of DMSO diluted in the same proportion as the corresponding emodin. Three parallel wells are set up in each group. After continuing to cultivate for 48 h, observe the cell state using an inverted optical microscope. After the cell culture is completed, centrifuge at 1000r/min for 10 min, aspirate and discard the culture medium, and add a mixture of 100 μL serum-free DMEM medium and 5 mg/mL MTT in a volume ratio of 9:1 to each well. Continue to culture for 4 h. After terminating the culture, centrifuge at 1500 r/min for 8 min, carefully remove the upper layer of liquid, add 150 μL DMSO to each well, shake at low speed for 10 min on a shaker to completely dissolve the crystals, measure the optical density (OD) of each well at a wavelength of 490 nm on an enzyme-linked immunosorbent assay (ELISA) reader, and calculate the cell proliferation inhibition rate (R) according to formula (1). A microplate reader measured the absorbance value of each well at 490 nm, and subsequently, the cell proliferation inhibition rate and half-maximal inhibitory concentration (IC_{50}) were computed using GraphPad Prism 9 software.

$$R = (1 - \text{OD}_{\text{experiment}} / \text{OD}_{\text{control}}) \times 100\% \quad (1)$$

2.10.3 RT-PCR validation of mRNA expression of signaling pathway related genes

Cells were seeded in 6-well cell culture plates at 2×10^5 cells/mL, with 2 mL per well. After complete cell adhesion, the experimental group was treated with 100 μL of active compound/active extract to achieve a final concentration of 20 $\mu\text{g/L}$. The control group was treated with DMSO diluted in the same proportion as the active compound which named EM. Three wells were set up in each group. After 48 h of cultivation, collect the cells, centrifuge at 1000 r/min for 8 min, discard the supernatant culture medium, wash three times with 3 mL of pre-cooled PBS, add $1 \times$ binding buffer to suspend the cells, and make the cell concentration 1×10^6 cells/mL.

After collecting cells, total RNA was extracted from each group of cells using the Trizol method, and the content and purity of RNA were measured using an ultra micro spectrophotometer. Take 1 μg of total RNA and synthesize cDNA according to the instructions of the first strand cDNA synthesis kit. Use this as a template for reverse

transcription-polymerase chain reaction (RT-PCR) amplification, with beta(β)-actin as the internal reference. The primer sequences used for the RT-PCR reaction are shown in Table 2. Amplification procedure: Pre-denaturation at 95 °C for 2 min, denaturation at 94 °C for 30 s, refolding at 60 °C for 1 min, extension at 72 °C for 60 s, and total extension at 72 °C for 10 min after 32 cycles. After the reaction, the PCR product is electrophoretic by 1% agarose gel, scanned and photographed by digital gel imaging, and analyzed the band.

2.10.4 Western blotting validation of protein expression of signaling pathway related genes

The Western blotting method was employed to assess the expression levels of proteins associated with anti-PCa. In the control group, 20 μ L of DMSO was administered to PC-3 cells. Conversely, PC-3 cells in the drug intervention group received 15 μ L of EM, with final concentrations varying at 10, 20, 40, 80, and 160 μ mol/L respectively. Following a 48 h incubation period, the cells were harvested on ice, and total protein extraction was conducted using the radio immuno precipitation assay (RIPA) lysis buffer assay kit for each group. Protein quantification was then performed using the bicinchoninic acid assay (BCA) assay, sourced from Wuhan Servicebio Technology Co., Ltd., China. Each protein sample, weighing 20 μ g, was denatured by heating at 100 °C for 12 min, separated via 10% sodium dodecyl sulfate -polyacrylamide gel electrophoresis (SDS-PAGE), and transferred onto polyvinylidene fluoride (PVDF) immobilon membranes.

For the Western blotting process, primary antibodies targeting rabbit/mouse/rat/human cysteine-aspartate protease 3 (CASP3, CAT. NO: YM8058), tumor necrosis factor (TNF, CAT. NO: YM3477), interleukin 1 beta (IL1B, CAT. NO: GB-122059), peroxisome proliferator-activated teceptor gamma (PPARG, CAT. NO: GB11164), human recombinant protein (MYC, CAT. NO: YM-8143), tumor protein 53 (TP53, CAT. NO: 10442-1-AP), and beta-actin (β -actin, CAT. NO: 66009-1-Ig) were used, each at a 1:5000 dilution. The secondary antibody utilized was goat anti-rabbit IgG (H + L) (CAT. NO: SA00001-2) and goat anti-mouse IgG (H + L) (CAT. NO: SA00001-1), at a 1:2000 dilution, sourced from Proteintech Group, Inc, China, Immunoway Co., Ltd, China, and Servicebio Tecnology Co., Ltd, China, respectively. The membranes were incubated with the corresponding primary antibody at room temperature for 1 h, followed by overnight incubation at 4°C. After washing the membranes, the secondary antibody was added, and the membranes were incubated on a shaking table for 2 h. Subsequently, the membranes were washed with TBST three times, with each wash lasting 10 min. The ECL imaging system was used for luminescent development. After replacing the membrane with a full one, the laboratory's costs increased substantially. As well as there are some labor costs need to be considered. When film cutting was the norm, a single film could be used to its maximum capacity, allowing for the detection of multiple indicators. Based on the above reasons, we generally use trimmed membranes to reduce labor and time costs. Therefore, trimmed membranes were finally used in the manuscript.

The experiment was repeated a minimum of three times, and the values obtained were measured and analyzed. The gray values of the bands were quantified using Image J 2.0 software (National Institutes of Health, <https://imagej.net/software/fiji/downloads>).

2.11 Statistical analysis

Statistical analysis was performed on all data using SPSS 21.0 software and GraphPad Prism 9.0, and the results were expressed as mean \pm standard deviation. Single factor analysis of variance was used for comparison between multiple groups, with $P < 0.05$ indicating statistically significant differences.

Table 2 Primers used for RT-PCR

Target genes	Primer sense (5'-3') Forward	Primer antisense (5'-3') Reverse
CASP3	GTGGAGGCCGACTTCTGTATGC	TGGCACAAAGCGACTGGATGAAC
TNF	GCTCCAGCGGTGCTTGTTTC	CCAGAGGGCTGATTAGAGAGAGGTC
IL1B	GGACAGGATATGGAGCAACAAGTGG	TCATCTTTCAACACGCAGGACAGG
TP53	GCCCATCCTACCATCATCACAC	GCACAAACACGCACCTCAAAGC
PPARG	TGAATCCAGAGTCCGCTGACCTC	ATCGCCCTCGCCTTTGCTTTG
MYC	AGCAGCGACTCTGAGGAGGAAC	TCCAGCAGAAGGTGATCCAGACTC

3 Results

3.1 Construction of “EM-PCa” regulatory network

EM is an anthraquinone with the molecular formula: $C_{15}H_{10}O_5$ (Fig. 1A). According to the search and screening of PCa target genes from Genecards database and DisGeNET database, a total of 323 PCa-related target genes were obtained. The intersection of EM target genes and PCa target genes and the Venn diagram were drawn. A total of 31

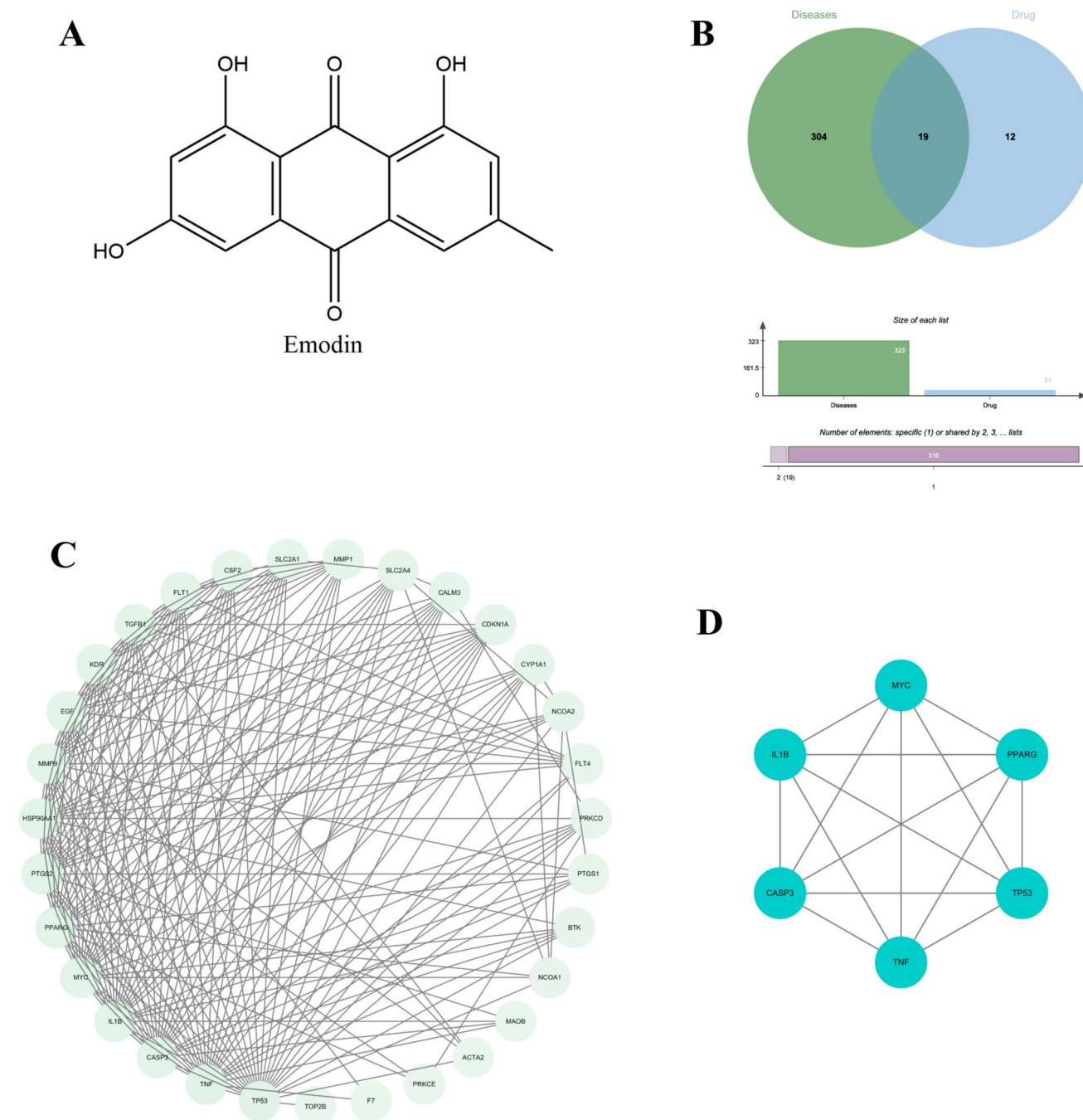


Fig. 1 **A** Chemical structure of emodin. **B** Venn diagram to screening of common target gene of EM and PCa-related targets. **C** PPI network of EM on anti-PCa. **D** Finally confirmed core targets of EM on anti-PCa

“EM-PCa” intersection genes were obtained. Perl software and TCMSP database were used to screen, and finally 19 EM related target genes were obtained (Fig. 1B).

3.2 PPI network construction and core target gene screening

The above gene information was uploaded to the STRING 11.1 database, and the species was selected as “Homo-sapiens”. The PPI network map was obtained and visualized by Cytoscape 3.7.2 software (Fig. 1C). Using “cytonca” plug-in, the core target genes were selected and a total of 6 potential core target genes were screened. Among them, the core target gene which including MYC, PPARG, TP53, TNF, CASP 3, IL1B ranked among the top 6 genes in degree (Table 3, Fig. 1D).

3.3 GO function enrichment analysis result

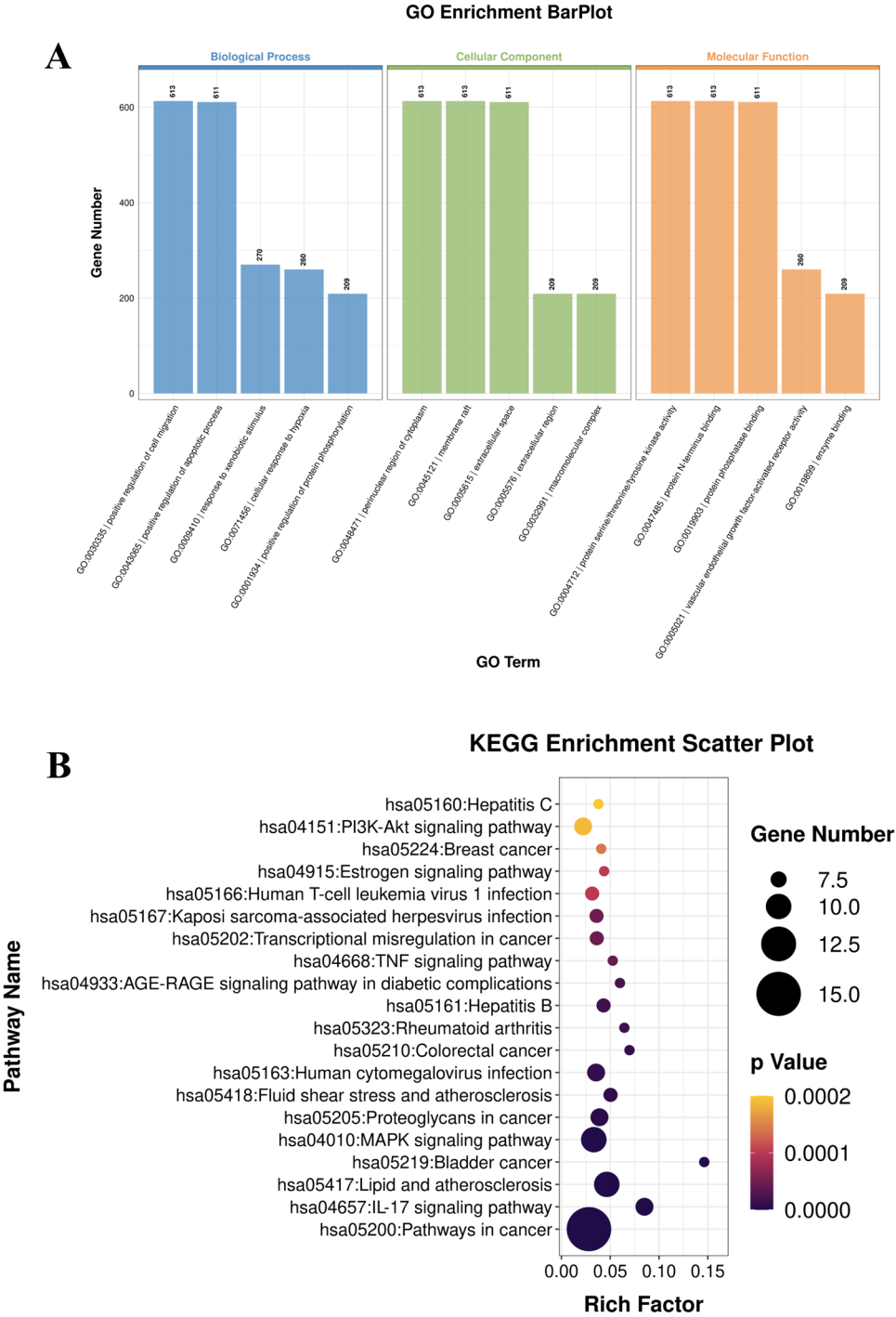
GO functional enrichment analysis was performed to obtain totally 410 functional entries. Select the top 5 items of biological processes (BP), cell components (CC) and Molecular functions (MF) to make a bar chart. Among them, BP mainly

Table 3 The betweenness centrality, closeness centrality and degree centrality of genes

Name of genes	Betweenness centrality	Closeness centrality	Degree centrality
TP53	0.14424662	0.88235294	26
TNF	0.09245347	0.85714286	25
IL1B	0.04269725	0.81081081	23
CASP3	0.04269725	0.81081081	23
MYC	0.03746684	0.78947368	22
PPARG	0.05947676	0.78947368	22
PTGS2	0.03664051	0.78947368	22
HSP90AA1	0.05103014	0.76923077	21
MMP9	0.02770248	0.75	20
EGF	0.03250191	0.73170732	19
TGFB1	0.01345947	0.69767442	17
KDR	0.01313189	0.69767442	17
FLT1	0.00380878	0.68181818	16
CSF2	2.74E-04	0.63829787	13
SLC2A1	9.50E-04	0.63829787	13
SLC2A4	0.00680519	0.625	12
MMP1	0	0.6122449	12
CALM3	0.00176618	0.6122449	11
CDKN1A	0	0.6122449	11
CYP1A1	0.00398636	0.58823529	9
NCOA2	0.00487875	0.57692308	9
PRKCD	0.00711665	0.57692308	8
FLT4	0	0.57692308	8
PTGS1	0.00136731	0.55555556	7
BTK	0	0.55555556	6
NCOA1	5.43E-04	0.53571429	6
ACTA2	0	0.50847458	4
MAOB	0	0.5	4
PRKCE	2.87E-04	0.48387097	3
F7	0	0.47619048	2
TOP2B	0	0.47619048	1

involve positive regulation of cell migration, positive regulation of apoptotic process, response to xenobiotic stimuli, cellular response to hypoxia, positive regulation of protein phosphorylation, etc. CC mainly involve perinuclear region of cytoplasm, membrane raft, extracellular space, extracellular region, macromolecular complex, etc. MF mainly involve protein serine kinase activity, protein N-terminus binding, protein phosphatase binding, vascular intrinsic growth factor active receptor activity, enzyme binding, etc. (Fig. 2A).

Fig. 2 **A** Bar diagram of GO functional enrichment analysis. **B** Bubble diagram of KEGG pathway enrichment analysis



3.4 KEGG pathway enrichment analysis result

The KEGG analysis results are shown in Fig. 2B, with 52 pathways associated with 29 potential genes. Enrichment analysis of the top 20 pathways revealed that hsa05160: hepatitis C, Hsa04151: PI3K-Akt signaling pathway, hsa05224: breast cancer, hsa04915: estrogens signaling pathway, hsa05166: human T-cell leukemia virus 1 infection, hsa05167: Kaposi sarcoma associated herpes virus infection, hsa05202: transcriptional misregulation in cancer, hsa04668: TNF signaling pathway, hsa04933: AGE-RAGE signaling pathway in diabetic complications, hsa05161: hepatitis B, hsa05323: rheumatoid arthritis, hsa05210: colorectal cancer, hsa05163: human cytomegalovirus infection, hsa05418: fluid shear stress and atherosclerosis, hsa05205: proteoglycans in cancer, hsa04010: mapk signaling pathway, hsa05219: bladder cancer, hsa05417: lipid and atherosclerosis, hsa04657: IL-17 signaling pathway, Hsa05200: pathways in cancer. are the main enriched pathways of key gene targets, suggesting that EM may play an anti-PCa role through multiple pathways. Annotated map of EM on PCa-related signaling pathways were presented in Fig. 3. According to DAVID database, the two pathways with the most enriched core genes were pathways in cancer (Fig. 3A) and IL-17 signaling pathway (Fig. 3B) respectively, and it was revealed that the above 6 core genes were highly expressed in the above two pathways.

3.5 Docking and visualization of EM with core target molecules

In order to verify the possibility that EM exerts anti-PCa effects through potential targets which including MYC, PPARG, TP53, TNF, CASP3, IL1B were used as receptor proteins (the top 6 core targets were screened out by cytonca topology analysis). The molecular docking analysis and visualization of EM with the 6 core targets were carried out by PyMOL 2.4.0 and Discovery Studio 2019 software (Fig. 4). Under the optimal mode, the docking energies of EM with MYC, PPARG, TP53, TNF, CASP3, and IL1B were -4.55 kcal/mol, -9.09 kcal/mol, -9.48 kcal/mol, -5.19 kcal/mol, -5.43 kcal/mol, -5.25 kcal/mol respectively (Table 4). EM formed hydrogen bonds with GLN-283 and CYS-285 of CASP3; formed hydrogen bonds with LEU-80 of IL1B; forms hydrogen bonds with DC-110, GLU-910, ARG-913 of MYC; forms hydrogen bonds with HIS-449, TYR-473, SER-289 of PPARG; forms carbon bonds with GLY-121 and GLY-122 of TNF respectively. EM forms a hydrogen bond with GLU-1761 of TP53. The molecular docking results showed that the active ingredient EM could be well docked with the predicted 6 core targets, verifying the possibility of EM regulating PCa.

3.6 Result of molecular dynamics simulation

Molecular dynamics simulations were performed using Discover Studio 2019 software. To predict the binding affinity between EM and the protein with the highest degree value (TP53) protein, a TP53/emodin structural complex model was constructed (Fig. 5A). Furthermore, molecular dynamics studies were undertaken to validate the stability of receptor-ligand complexes, achieved through a comprehensive analysis of diverse parameters. Root mean square deviation (RMSD) and root mean square fluctuation (RMSF) are two widely utilized parameters in molecular dynamics simulations and related fields. RMSD primarily serves to quantify the difference between two structures and evaluate the stability of the system, while RMSF describes the dynamic fluctuations within the internal structure of a molecule. Upon initiation of the molecular dynamics simulation, the total energy predominantly fluctuates around $-149,750$ kcal/mol (Fig. 5B), with the RMSD value oscillating near 0.825 and tending towards a constant value (Fig. 5C). Meanwhile, the RMSF value fluctuates around 15 (Fig. 5D), indicating a stable hydrogen bonding pattern as reflected in the hydrogen bond heatmap (Fig. 5E), where most small molecule ligands exhibit stable hydrogen bonding with the receptor protein. This suggests that during the simulation, the small molecule eventually converges to a stable, most populated conformational cluster after exhibiting multiple conformational changes. Both main chains RMSF and side chains RMSF are essential analytical tools in molecular dynamics simulations, portraying the dynamic fluctuations of the protein main chains and side chains, respectively. In the present study, the fluctuations observed in both main chains RMSF and side chains RMSF correlate well with the corresponding hydrogen bond and amino acid profiles (Fig. 5F). By analyzing these parameters, it was revealed that the amino acid residues interacting with EM remain relatively stable, confirming the stable binding of EM within the substrate-binding pocket of TP53 protein. Researchers can gain profound insights into protein stability, function, and interaction mechanisms with other molecules, thereby providing valuable support for drug design and other related research endeavors.

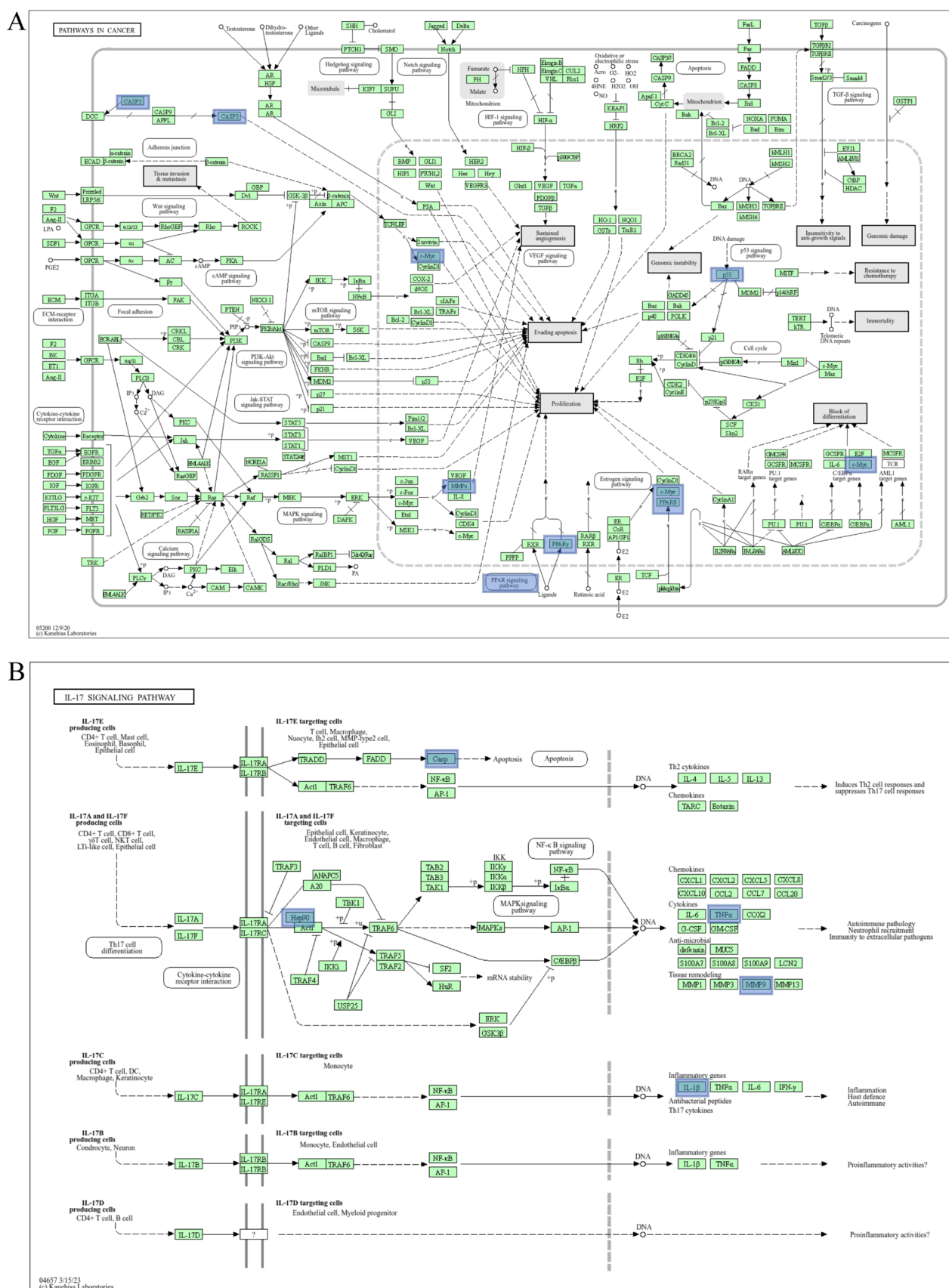


Fig. 3 Annotated map of EM on PCa-related signaling pathways. **A** Cancer signaling pathway. **B** IL-17 signaling pathway



Compound	Target	PDB	Energy (kcal/mol)
emodin	MYC	1nkp	− 4.55
emodin	PPARG	1knu	− 9.09
emodin	TP53	1dt7	− 9.48
emodin	TNF	2az5	− 5.19
emodin	CASP3	1re1	− 5.43
emodin	IL1B	1s0l	− 5.25

GEPIA database was used to determine the mRNA expression levels of MYC, PPARG, TP53, TNF, CASP3, IL1B in PCa and normal patients. Among them, 492 cases of PCa tissues and 152 cases of normal prostate tissues were taken as the research objects. Compared with normal prostate tissue, the expression level of CASP3 in PCa tissue was significantly increased ($P < 0.05$), while there was no significant difference in the mRNA expression of MYC, PPARG, TP53, TNF, IL1B (Fig. 6A). Hazard ratio (HR) represents the relative hazard ratio of death per unit time between the test group and the control group throughout the follow-up time. HR less than 1 represents a reduction in the risk of death per unit time, and HR greater than 1 represents an increase in the risk of death per unit time. The HR is equal to 0.5, which can be considered as a 50% reduction in the risk of death per unit time. In tumor research, HR is an evaluation standard of recurrence risk. Generally,

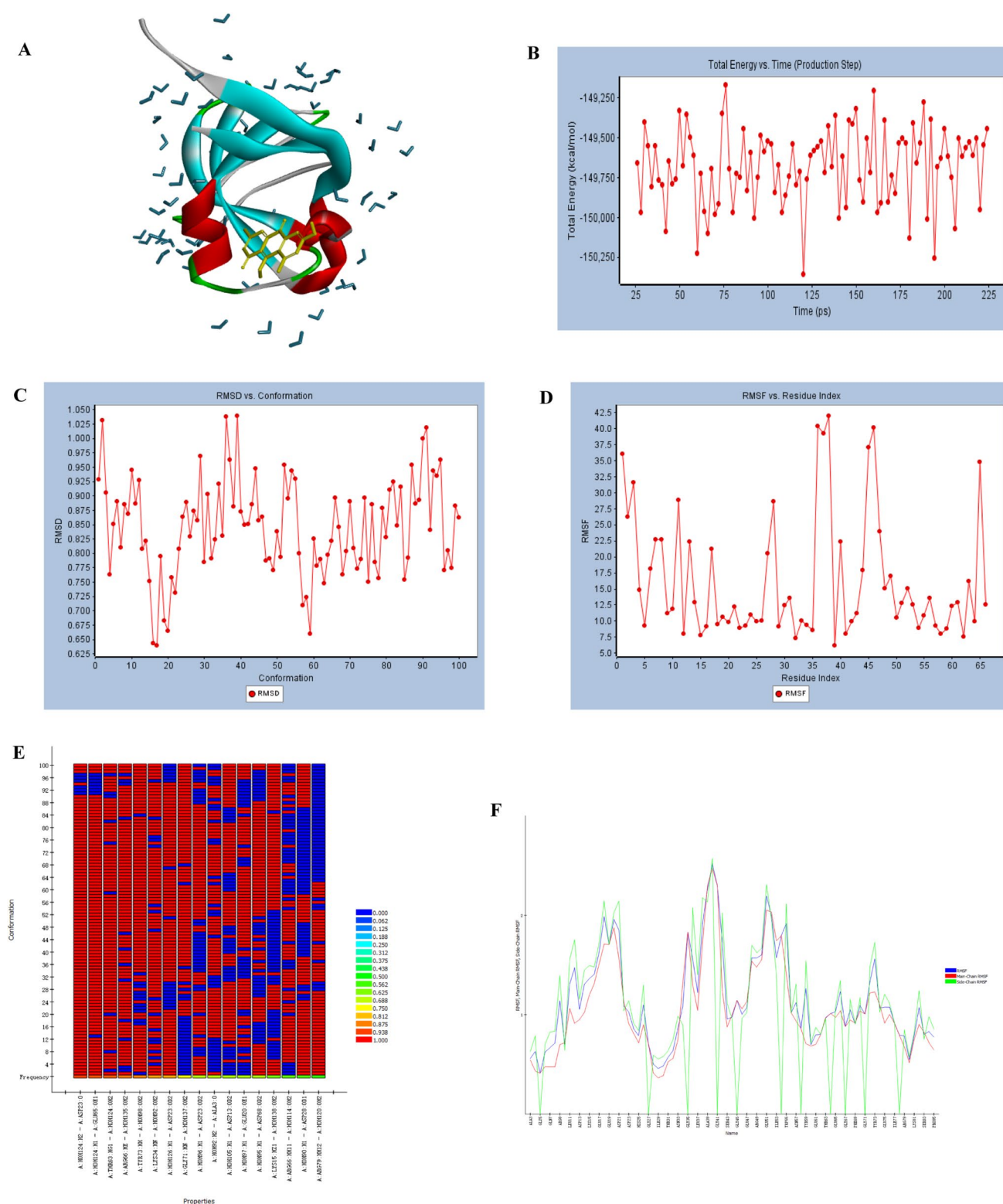


Fig. 5 **A** TP53/emodin structural complex model. **B** The total energy of molecular dynamics simulation. **C** RMSD value. **D** RMSF value. **E** Hydrogen bond heatmap. **F** The dynamic fluctuations of the protein main chains and side chains

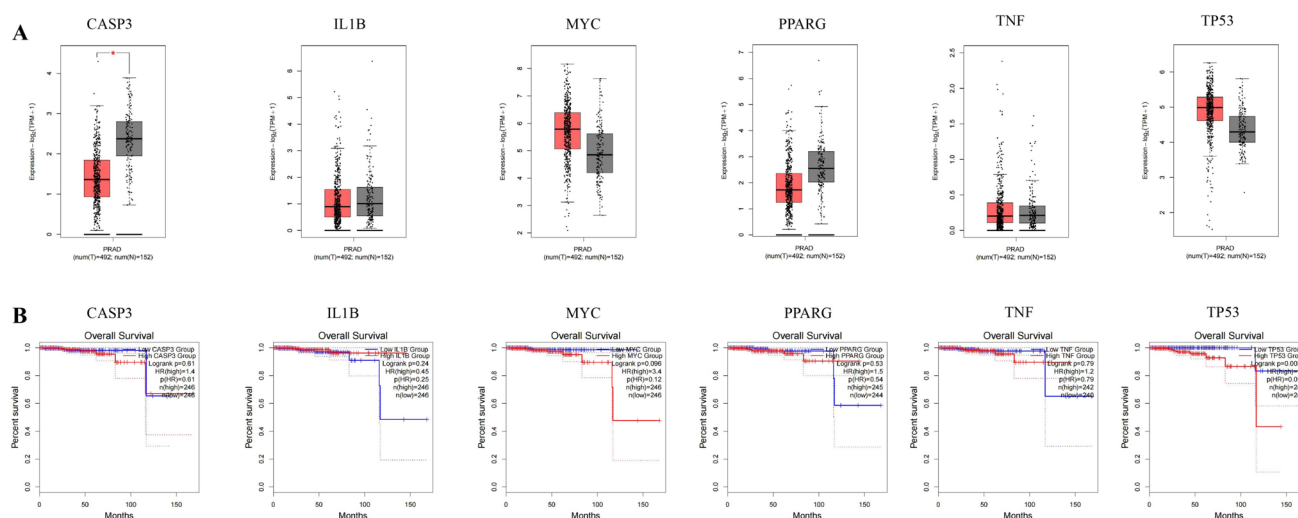


Fig. 6 **A** The mRNA expression levels of CASP3, IL1B, MYC, PPARG, TNF, TP53 in PCa patients. **B** The survival curve of CASP3, IL1B, MYC, PPARG, TNF, TP53 in PCa patients

the higher the HR value, the greater the recurrence risk of patients; the lower the HR value, the lower the risk of recurrence. Clinically, HR is generally regarded as one of the indicators to judge the prognosis of patients with PCa. According to different molecular types and pathological stages, the recurrence risk of patients can be accurately predicted, and the corresponding treatment plan can be formulated. Kaplan–meier plotter online database was used to evaluate the effect of different expressed core genes on the prognosis of PCa patients. Patients with high expression of IL1B (HR=0.45) had better OS than those with low expression, while patients with low expression of other genes MYC (HR=3.4), PPARG (HR=1.5), TP53 (HR=12), TNF (HR=1.2), CASP3 (HR=1.4) had better OS than those with high expression (Fig. 6B).

3.8 Effect of emodin on the viability of PC-3 cells

To investigate the effect of EM on the survival rate of PC-3 cells, cells were treated with different concentrations (0.1 ~ 1.6 $\mu\text{mol/L}$) of EM for 48 h, and cell viability was detected by MTT assay. The IC_{50} was calculated and the value is 0.1906 $\mu\text{mol/L}$. As shown in Fig. 7A, B, compared with the control group, treatment with EM at concentrations of 0.4 ~ 1.6 $\mu\text{mol/L}$ may significantly reduced the survival rate of PC-3 cells ($P < 0.05$) which indicating that EM has a significant inhibitory effect on PC-3 cells.

3.9 Result of RT-PCR

To study the effect of emodin on anti-PCs, the mRNA levels of CASP3, TNF, IL1B, TP53, PPARG, and MYC in PC-3 cells were evaluated by RT-PCR method. The increased mRNA expressions of CASP3 (0.4 ~ 1.6 $\mu\text{mol/L}$), and PPARG (0.2 ~ 1.6 $\mu\text{mol/L}$) in PC-3 cells were significantly higher in different concentrations emodin treatment group than those in the control group ($P < 0.05$). The increased mRNA expressions of TNF (0.4 ~ 1.6 $\mu\text{mol/L}$), TP53 (0.1 ~ 1.6 $\mu\text{mol/L}$), and MYC (0.2 ~ 1.6 $\mu\text{mol/L}$) were significantly lower in different concentrations emodin treatment group than those in the control group ($P < 0.05$). The mRNA expressions of IL1B was no significant changes (Fig. 7C). The present study showed that EM may play an important role in reducing the growth of PC-3 cells via increased mRNA expressions of CASP3, PPARG and decreased mRNA expressions of TNF, TP53, MYC.

3.10 Result of western blot

In order to investigate the mechanism of EM's anti-PCa effect, the present study ultimately examined the protein expression levels of CASP3, TNF, IL1B, TP53, PPARG, and MYC. When compared to the control group, Emodin significantly increased protein expressions of CASP3 (40 ~ 160 $\mu\text{mol/L}$), PPARG (20 ~ 160 $\mu\text{mol/L}$) and decreased protein expressions of TNF (40 ~ 160 $\mu\text{mol/L}$), IL1B (80 $\mu\text{mol/L}$), TP53 (40 ~ 160 $\mu\text{mol/L}$), MYC (40 ~ 160 $\mu\text{mol/L}$) ($P < 0.05$) (Fig. 8A, B).

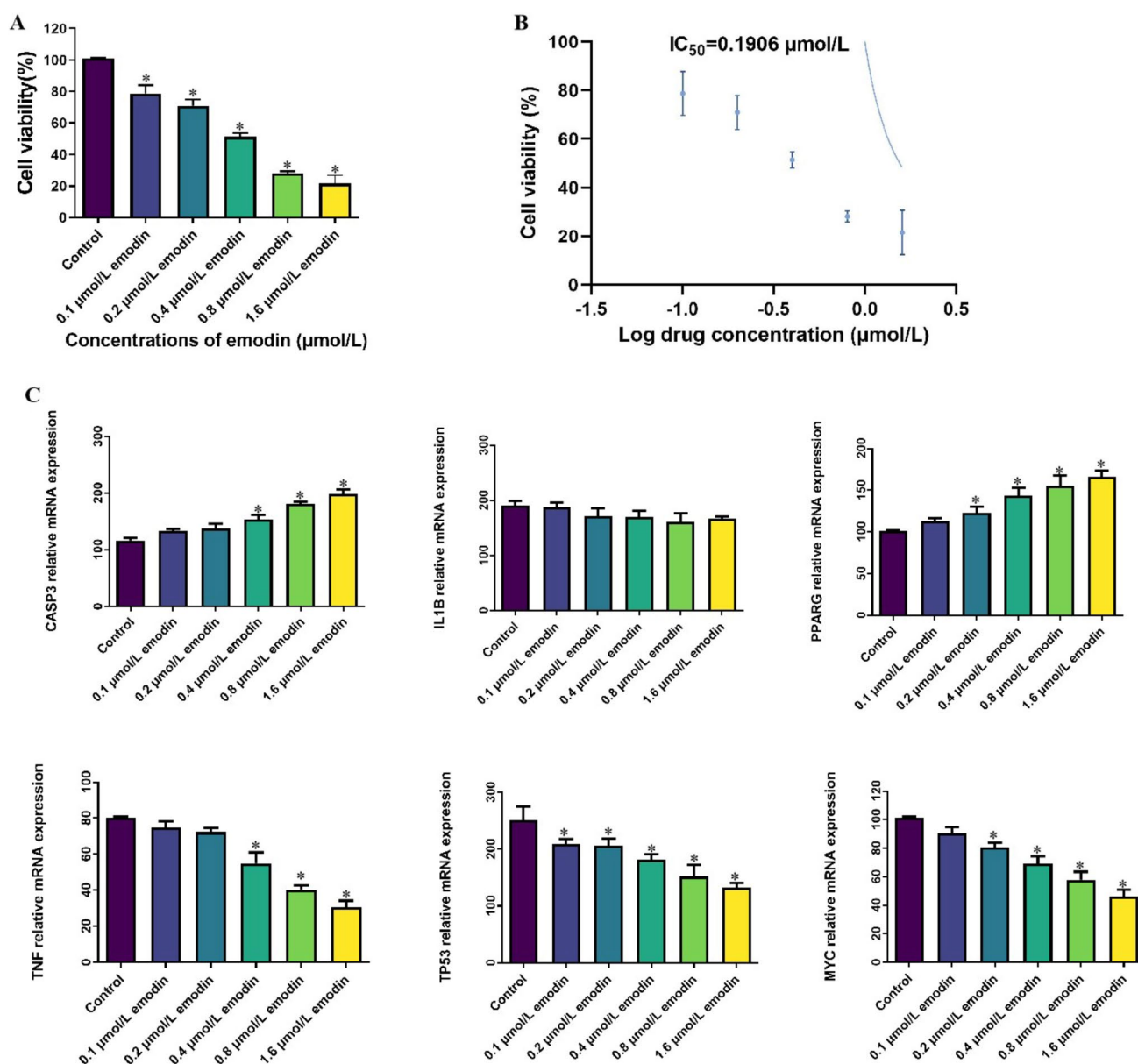


Fig. 7 Effect of EM on PC-3 cells. **A, B** Effect of EM on cell viability. Cells were treated with different concentrations of EM for 48 h. **C** Effect of EM on CASP3, IL1B, PPARG, TNF, TP53, and MYC mRNA levels in PC-3 cells. Data were presented as the mean \pm SD values performed in triplicate (* $P < 0.05$ vs. Control group)

4 Discussion

PCa is the second most common cancer worldwide, with more than 1.1 million new cases each year, accounting for approximately 15% of all confirmed cancers, and is the second leading cause of cancer-related death in men [28, 29]. The prevalence and incidence of PCa vary all over the world, with the highest in Europe and America and the lowest in Asia [30]. In recent years, due to the global population growth and aging, as well as changes in lifestyle and dietary patterns, the incidence of PCa has shown an upward trend, and even in regions with low incidence in the past, such as Asia, especially northeast Asia, has also increased significantly [31]. PCa can be divided into two types, including hormone dependent type and castration resistant type. Initially, hormone treatment of PCa has a significant effect, but after the first androgen removal treatment, the disease will continue to recur or even metastasize to other tissues or organs. At this time, it is called castration resistant PCa. This type of PCa is usually insensitive to anticancer drugs [2]. Clinically, PCa

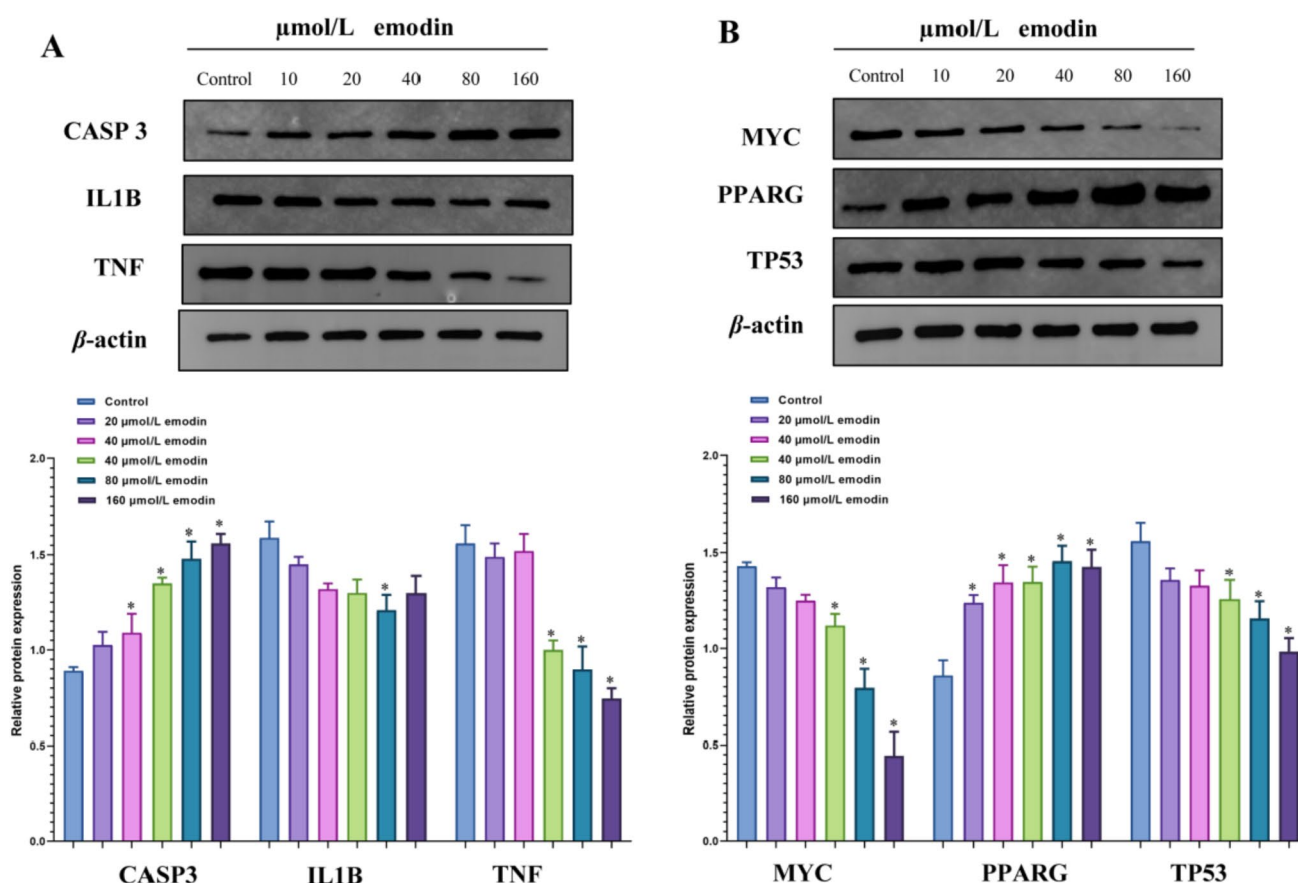


Fig. 8 Effect of EM on CASP3, IL1B, PPARG, TNF, TP53, and MYC protein levels in PC-3 cells. **A** The protein expressions of CASP3, IL1B, and TNF. **B** The protein expressions of MYC, PPARG and TP53. Data were presented as the mean \pm SD values performed in triplicate (* P < 0.05 vs. Control group)

is meticulously categorized into four distinct stages, based on the extent of invasion and dissemination. Stage I and II cancers remain localized within the confines of the prostate gland, demonstrating minimal progression beyond its borders. Conversely, Stage III cancer exhibits a more advanced pattern, extending its reach to adjacent tissues, including those surrounding the prostate or seminal vesicles. Notably, at this stage, the cancer does not penetrate into neighboring organs or infiltrate lymph nodes, nor does it metastasize to distant sites. Finally, stage IV cancer signifies a profound progression, characterized by the dissemination of tumors to both adjacent and distant organs, as well as to lymph nodes, underscoring the need for aggressive therapeutic intervention [32].

It was shown that monomer derives from TCM exhibits an obvious advantages in inhibiting the activity of tumor cells, because it can not only inhibit and kill tumor cells, but also reduce the adverse reactions of radiotherapy and chemotherapy. It can also improve the quality of life and immunity of cancer patients, reduce clinical symptoms and prolong survival time [33]. Previous study have shown that 5 ~ 20 mg/kg EM intraperitoneal injection may exert anti-inflammatory effects by regulating granulocyte function in rats with acute lung injury [34]. EM also play an anti-inflammatory role in acute lung injury by regulating JNK/ nerve growth factor induced gene B (Nur77) /c-Jun[35], inhibiting mammalian target of rapamycin (mTOR)/ hypoxia inducible factor-1 α (HIF-1 α) / vascular endothelial growth factor (VEGF) signaling pathway [36], and inhibiting the production of inflammatory factors and oxidative stress in mouse macrophage RAW264.7. It was reported that EM may regulates immune function by inhibiting toll like receptor 3 (TLR3) pathway [37]. In addition, EM inhibits apoptosis by mediating bcl-2-associatedx protein (bax) /bcl2/casp3 pathway, regulates the proportion of T cells, protects the intestinal barrier and inhibits the immune response in severe acute pancreatitis [25]. EM treatment of rat chondrocytes for 2 h could reduce IL-1 β induced cytotoxicity, inhibit the expression of nitrogen monoxide (NO), prostaglandin E2 (PGE2), matrix metalloproteinase (MMP)-3 and MMP-13 and extracellular regulated protein kinases (ERK) and wingless-type MMTV integration site family member (wnt) / β -catenin pathways, and ultimately promote the proliferation of chondrocytes [38]. EM can activate p53 and induce apoptosis of hepatic stellate cells through the p53/ERK/p38

axis, and remodel the extracellular matrix to improve liver fibrosis by regulating MMP-1 and MMP-9 [39]. However, the research on PCa is only limited to the cellular level, and the research on pathways and related targets is not deep enough.

GO enrichment analysis confirmed that EM has a certain impact on several biological processes, such as positive regulation of cell migration, positive regulation of apoptotic process, perinuclear region of cytoplasmic, membrane raft, protein serine kinase activity, protein N-terminus binding, etc. In addition, KEGG enrichment analysis showed that the key targets of EM mainly involved signaling pathways such as hepatitis C, PI3K-Akt, IL-17, MAPK, estrogens, pathways in cancer, etc. The key targets of EM are enriched in these pathways, especially the IL-17 and pathways in cancer pathways. Previous reports have shown that IL-17 can activate and regulate the proliferation, migration and apoptosis of tumor cells, and induce the formation of other tumor factors in vitro [40]. It indicates that EM exert its anti-tumor effect with the help of these targets and signaling pathways, and these pathways and key targets may become the direction of further exploring the anti-tumor mechanism of EM in the future.

In the PPI network, the top 6 core targets with degree values mainly including MYC, PPARG, TP53, TNF, CASP3, IL1B. There are many signal pathways associated with it, which play an important role in the regulation of tumor. Among them, previous studies have shown that the proto-oncogene transcription factor c-MYC is overexpressed in the early stage of PCa, which will induce comprehensive metabolic reprogramming to support the survival and proliferation of cancer cells. It was considered to a key driver of the occurrence and development of PCa, and is closely related to the metastatic progress and poor prognosis of PCa [41]. C-MYC is intertwined with a large number of gene alterations and signaling defects observed in PCa. For example, Transmembrane protease, serine 2 (TMPRSS2)-E26-related gene (ERG) gene fusion can increase the level of c-MYC protein, and phosphatase and tensin homolog (PTEN)/Trp53 deletion is caused by the dysregulation of c-MYC protein expression [42]. The study also found that c-MYC regulates 7 differentially expressed proteins, including glucose regulated protein (GRP) 78 and heat shock protein (HSP) 60, and participates in biological pathways involving anti apoptosis and regulation of caspase activity, indicating that c-MYC plays an important role in regulation of PCa. Casp3, belonging to the esteemed class of proteolytic enzymes, serves as a pivotal mediator of apoptosis, the orchestrated cell death process. Renowned as a key effector enzyme among the caspase family, it assumes a paramount role as an indispensable effector molecule, instrumental in the meticulous execution of apoptosis. Furthermore, casp3 belongs to the exclusive cysteinyl aspartate-specific protease family, underscoring its specificity and significance in regulating programmed cell death [43]. Under normal conditions, intracellular casp3 exists as an inactive zymogen and is activated as active casp3 only when cells are apoptotic [44]. Previous studies have found that casp3 expression in BPH tissues is mainly in secretory epithelial cells, while only a small amount is expressed in basal cells [45]. Another study also showed that the positive expression rate of casp3 in PCa tissues was also significantly lower than that in non tumor tissues [46]. TP53 is the most frequently mutated gene in cancer. Sun et al. analyzed the mutation proportion of TP53 in a large sample of population in the database by bioinformatics method based on public databases, and the result showed that the mutation rate of TP53 in PCa was 18% [47]. Aizoubi et al. performed exome sequencing on 79 PCa specimens after radical prostatectomy and found that the mutation rate of TP53 was 13.9% [48]. It indicates that the mutation rate of this gene is closely related to PCa. TNF is mainly synthesized and secreted by macrophages, and plays the function of regulating immunity in the human body, with anti infection, anti-inflammatory and anti-virus effects [49]. Under standard conditions, this index functions as a potent inhibitor, preventing the abnormal proliferation and malignant transformation of tissue cells, while simultaneously exerting inhibitory and cytotoxic effects on tumor cells. However, intriguing clinical findings have revealed that TNF- α , paradoxically, can also facilitate the malignant progression of tumors, highlighting the complexity of its biological roles [50, 51]. The molecular docking and molecular dynamics results showed that EM had good affinity with the core targets, providing the possibility of EM exerting anti-PCa effect through these key targets.

Study limitations as following: although emodin, as a natural medicinal ingredient with significant anti-tumor activity, has shown broad application prospects in the treatment of prostate cancer, its clinical translation still faces some challenges. For example, the poor water solubility of emodin leads to its low bioavailability. Emodin may interact with certain drugs when used in combination, and when used in combination with antibiotics, it may affect the absorption or metabolism of antibiotics. When used in combination with anticoagulant drugs, there may be an increased risk of bleeding as emodin may have an impact on coagulation function. So in clinical use, attention should be paid to the compatibility with other drugs.

In addition, at certain doses, emodin may cause gastrointestinal reactions such as nausea, vomiting, diarrhea, etc. This is mainly because emodin has a laxative effect, and excessive use can stimulate the gastrointestinal tract, leading to gastrointestinal dysfunction. Long term or extensive use may also affect the balance of normal gut microbiota. Therefore, further research is needed on the metabolism and excretion process of emodin in the body. To address these issues,

researchers are exploring various strategies, such as changing the mode of administration, developing new formulations, etc., to improve the clinical efficacy and safety of emodin.

5 Conclusion

Taken together, the present study explored the potential targets and action pathways of EM in regulating PCa through network pharmacology, and screened out 6 related targets (MYC, PPARG, TP53, TNF, CASP3, IL1B) with anti-PCa effects. Among them, the level of CASP3 protein expression was notably higher in healthy individuals compared to those suffering from prostate cancer, while the expression of TP53 protein demonstrated a strong correlation with the survival rates of prostate cancer patients. The pathways in cancer and IL-17 signaling pathway were the key pathways in regulation of PCa. The experimental verification results showed that treatment with 0.4 ~ 1.6 $\mu\text{mol/L}$ EM significantly reduced the survival rate of PC-3 cells ($P < 0.05$), and emodin may have a significant inhibitory effect on PC-3 cells by increasing the mRNA expression of CASP3, and PPARG and decreasing the mRNA expression of TNF, TP53, and MYC respectively. The above results clarify the potential role and molecular mechanism of EM in the treatment of PCa, and provide a basis for the development of new drugs for the treatment of PCa. In addition, according to different molecular types and pathological stages, the recurrence risk of patients might be accurately predicted and the corresponding treatment plan can be formulated.

Acknowledgements We gratefully acknowledge the contributions of TCMSP, DisGeNET, Genecards, LC-BIO, PubChem, GEPIA, and Kaplan Meier-plotter networks.

Author contributions G.Y. and JX. M. wrote the manuscript and created the figures, G.Y., Z. L., and JX. M. performed experiment, data analysis and revised critically the manuscript. All authors reviewed the manuscript.

Funding This work was financially supported by Key Scientific and Technological Research Project of Chongqing Municipal Education Commission (No. KJZD-K202302801), Scientific Research Project of Chongqing Medical and Pharmaceutical College (ygz2022104, ygzrc2024104, ygzzd2024101), Chongqing Municipal Education Commission Youth Project (KJQN202402816) and Science and Technology Bureau of Nan'an District, Chongqing (2024-20) respectively.

Data availability The data utilized in the present study can be sourced from publicly accessible databases. Additionally, datasets and raw images during the present study can be obtained from the corresponding author upon reasonable request.

Declarations

Ethics approval and consent to participate Not applicable.

Consent for publication Not applicable.

Competing interests The authors declare no competing interests.

Open Access This article is licensed under a Creative Commons Attribution-NonCommercial-NoDerivatives 4.0 International License, which permits any non-commercial use, sharing, distribution and reproduction in any medium or format, as long as you give appropriate credit to the original author(s) and the source, provide a link to the Creative Commons licence, and indicate if you modified the licensed material. You do not have permission under this licence to share adapted material derived from this article or parts of it. The images or other third party material in this article are included in the article's Creative Commons licence, unless indicated otherwise in a credit line to the material. If material is not included in the article's Creative Commons licence and your intended use is not permitted by statutory regulation or exceeds the permitted use, you will need to obtain permission directly from the copyright holder. To view a copy of this licence, visit <http://creativecommons.org/licenses/by-nc-nd/4.0/>.

References

1. Siegel RL, Miller KD, Jemal A. Cancer statistics, 2019. *CA Cancer J Clin.* 2019;69(1):7–34.
2. Feng RM, Zong YN, Cao SM, Xu RH. Current cancer situation in China: good or bad news from the 2018 Global Cancer Statistics? *Cancer Commun.* 2019;39(1):1–12.
3. Rawla P. Epidemiology of prostate cancer. *World J Oncol.* 2019;10(2):63.
4. Knura M, Garczor W, Borek A, Drzymala F, Rachwał K, George K, Francuz T. The influence of anti-diabetic drugs on prostate cancer. *Cancers.* 2021;13(8):1827.

5. Saranyutanon S, Srivastava SK, Pai S, Singh S, Singh AP. Therapies targeted to androgen receptor signaling axis in prostate cancer: progress, challenges, and hope. *Cancers*. 2019;12(1):51.
6. Song J, Chen W, Zhu G, Wang W, Sun F, Zhu J. Immunogenomic profiling and classification of prostate cancer based on HIF-1 signaling pathway. *Front Oncol*. 2020;10:1374.
7. Johns LE, Houlston RS. A systematic review and meta-analysis of familial prostate cancer risk. *BJU Int*. 2003;91(9):789–94.
8. Zhang Y, Fu Y. Comprehensive analysis and identification of an immune-related gene signature with prognostic value for prostate cancer. *Int J General Med*. 2021;14:2931–42.
9. Selnaes KM, Krüger-Stokke B, Elschot M, Johansen H, Steen PA, Langørgen S, et al. Detection of recurrent prostate cancer with 18F-fluciclovine PET/MRI. *Front Oncol*. 2020;10: 582092.
10. Byun SJ, Kim YS, Ahn H, Kim CS. Image-guided, whole-pelvic, intensity-modulated radiotherapy for biochemical recurrence following radical prostatectomy in high-risk prostate cancer patients. *PLoS ONE*. 2018;13(1): e0190479.
11. Tseng CS, Wang YJ, Chen CH, Wang SM, Huang KH, Chow PM, et al. Outcomes and prediction models for exclusive prostate bed salvage radiotherapy among patients with biochemical recurrence after radical prostatectomy. *Cancers*. 2021;13(11):2672.
12. Nakazawa M, Paller C, Kyprianou N. Mechanisms of therapeutic resistance in prostate cancer. *Curr Oncol Rep*. 2017;19:1–12.
13. Hwang C. Overcoming docetaxel resistance in prostate cancer: a perspective review. *Ther Adv Med Oncol*. 2012;4(6):329–40.
14. Wang J, Ding R, Ouyang T, Gao H, Kan H, Li Y, et al. Systematic investigation of the mechanism of herbal medicines for the treatment of prostate cancer. *Aging (Albany NY)*. 2023;15(4):1004.
15. Tang T, Yin L, Yang J, Shan G. Emodin, an anthraquinone derivative from *Rheum officinale* Baill, enhances cutaneous wound healing in rats. *Eur J Pharmacol*. 2007;567(3):177–85.
16. Saunders IT, Mir H, Kapur N, Singh S. Emodin inhibits colon cancer by altering BCL-2 family proteins and cell survival pathways. *Cancer Cell Int*. 2019;19:1–15.
17. Zhang N, Wang J, Sheng A, Huang S, Tang Y, Ma S, Hong G. Emodin Inhibits the proliferation of MCF-7 human breast cancer cells through activation of aryl hydrocarbon receptor (AhR). *Front Pharmacol*. 2021;11: 622046.
18. Li M, Jin S, Cao Y, Xu J, Zhu S, Li Z. Emodin regulates cell cycle of non-small lung cancer (NSCLC) cells through hyaluronan synthase 2 (HA2)-HA-CD44/receptor for hyaluronic acid-mediated motility (RHAMM) interaction-dependent signaling pathway. *Cancer Cell Int*. 2021;21:1–12.
19. Tong H, Huang Z, Chen H, Zhou B, Liao Y, Wang Z. Emodin reverses gemcitabine resistance of pancreatic cancer cell lines through inhibition of IKK β /NF- κ B signaling pathway. *OncoTargets Therapy*. 2020;9839–9848.
20. Zhang FY, Li RZ, Xu C, Fan XX, Li JX, Meng WY, et al. Emodin induces apoptosis and suppresses non-small-cell lung cancer growth via downregulation of sPLA2-IIa. *Phytomedicine*. 2022;95:153786.
21. Deng G, Ju X, Meng Q, Yu ZJ, Ma LB. Emodin inhibits the proliferation of PC3 prostate cancer cells in vitro via the Notch signaling pathway. *Mol Med Rep*. 2015;12(3):4427–33.
22. Cha TL, Qiu L, Chen CT, Wen Y, Hung MC. Emodin down-regulates androgen receptor and inhibits prostate cancer cell growth. *Can Res*. 2005;65(6):2287–95.
23. Tu Y, Wu Z, Tan B, Yang A, Fang Z. Emodin: its role in prostate cancer-associated inflammation. *Oncol Rep*. 2019;42(4):1259–71.
24. Liu K, Park C, Li S, Lee KW, Liu H, He L, et al. Aloe-emodin suppresses prostate cancer by targeting the mTOR complex 2. *Carcinogenesis*. 2012;33(7):1406–11.
25. Zhou Q, Xiang H, Liu H, Qi B, Shi X, Guo W, et al. Emodin alleviates intestinal barrier dysfunction by inhibiting apoptosis and regulating the immune response in severe acute pancreatitis. *Pancreas*. 2021;50(8):1202–11.
26. Ye Y, Zhong W, Luo R, Wen H, Ma Z, Qi S, et al. Thermosensitive hydrogel with emodin-loaded triple-targeted nanoparticles for a rectal drug delivery system in the treatment of chronic non-bacterial prostatitis. *J Nanobiotechnol*. 2024;22(1):33.
27. Mao J, Tang L, Fang L, Tian C, Zhu Z, Li Y. Systematic pharmacology-based strategy to explore the mechanism of Semen Strychni for treatment of papillary thyroid carcinoma. *Sci Rep*. 2023;13(1):18492.
28. Chi KN, Kheoh T, Ryan CJ, Molina A, Bellmunt J, Vogelzang NJ, et al. A prognostic index model for predicting overall survival in patients with metastatic castration-resistant prostate cancer treated with abiraterone acetate after docetaxel. *Ann Oncol*. 2016;27(3):454–60.
29. Moya L, Meijer J, Schubert S, Matin F, Batra J. Assessment of miR-98-5p, miR-152-3p, miR-326 and miR-4289 expression as biomarker for prostate cancer diagnosis. *Int J Mol Sci*. 2019;20(5):1154.
30. Krstev S, Knutsson A. Occupational risk factors for prostate cancer: a meta-analysis. *J Cancer Prev*. 2019;24(2):91.
31. Kimura T, Egawa S. Epidemiology of prostate cancer in Asian countries. *Int J Urol*. 2018;25(6):524–31.
32. Melegh Z, Oltean S. Targeting angiogenesis in prostate cancer. *Int J Mol Sci*. 2019;20(11):2676.
33. Zhong C, Wall NR, Zu Y, Sui G. Therapeutic application of natural medicine monomers in cancer treatment. *Curr Med Chem*. 2017;24(34):3681–97.
34. Mei H, Tao Y, Zhang T, Qi F. Emodin alleviates LPS-induced inflammatory response in lung injury rat by affecting the function of granulocytes. *J Inflamm*. 2020;17:1–13.
35. Xie P, Yan LJ, Zhou HL, Cao HH, Zheng YR, Lu ZB, et al. Emodin protects against lipopolysaccharide-induced acute lung injury via the JNK/Nur77/c-Jun signaling pathway. *Front Pharmacol*. 2022;13: 717271.
36. Li X, Shan C, Wu Z, Yu H, Yang A, Tan B. Emodin alleviated pulmonary inflammation in rats with LPS-induced acute lung injury through inhibiting the mTOR/HIF-1 α /VEGF signaling pathway. *Inflamm Res*. 2020;69:365–73.
37. Ding Y, Xu J, Cheng LB, Huang YQ, Wang YQ, Li H, et al. Effect of emodin on coxsackievirus B3m-mediated encephalitis in hand, foot, and mouth disease by inhibiting toll-like receptor 3 pathway in vitro and in vivo. *J Infectious Dis*. 2020;222(3):443–55.
38. Liu Z, Lang Y, Li L, Liang Z, Deng Y, Fang R, Meng Q. Effect of emodin on chondrocyte viability in an in vitro model of osteoarthritis. *Exp Ther Med*. 2018;16(6):5384–9.
39. Liang B, Gao L, Wang F, Li Z, Li Y, Tan S, et al. The mechanism research on the anti-liver fibrosis of emodin based on network pharmacology. *IUBMB Life*. 2021;73(9):1166–79.
40. Fabre J, Giustiniani J, Garbar C, Antonicelli F, Merrouche Y, Bensussan A, et al. Targeting the tumor microenvironment: the protumor effects of IL-17 related to cancer type. *Int J Mol Sci*. 2016;17(9):1433.

41. Labbé DP, Zadra G, Yang M, Reyes JM, Lin CY, Cacciatore S, et al. High-fat diet fuels prostate cancer progression by rewiring the metabolome and amplifying the MYC program. *Nat Commun.* 2019;10(1):4358.
42. Labbé DP, Brown M. Transcriptional regulation in prostate cancer. *Cold Spring Harb Perspect Med.* 2018;8(11): a030437.
43. Karki P, Lee J, Shin SY, Cho B, Park IS. Kinetic comparison of procaspase-3 and caspase-3. *Arch Biochem Biophys.* 2005;442(1):125–32.
44. Roy S, Bayly CI, Gareau Y, Houtzager VM, Kargman S, Keen SL, et al. Maintenance of caspase-3 proenzyme dormancy by an intrinsic “safety catch” regulatory tripeptide. *Proc Natl Acad Sci.* 2001;98(11):6132–7.
45. Bozec A, Ruffion A, Decaussin M, Andre J, Devonec M, Benahmed M, Mauduit C. Activation of caspases-3,-6, and-9 during finasteride treatment of benign prostatic hyperplasia. *J Clin Endocrinol Metab.* 2005;90(1):17–25.
46. Winter RN, Kramer A, Borkowski A, Kyprianou N. Loss of caspase-1 and caspase-3 protein expression in human prostate cancer. *Can Res.* 2001;61(3):1227–32.
47. Sun J, Zhang K, Cai Z, Li K, Zhao C, Fan C, Wang J. Identification of critical pathways and hub genes in TP53 mutation prostate cancer by bioinformatics analysis. *Biomark Med.* 2019;13(10):831–40.
48. Al Zoubi MS, Otoum R, Alorjani MS, Al Bashir S, Al Trad B, Abualrja MI, et al. TP53, SPOP and PIK3CA genes status in prostate cancer. *Asian Pac J Cancer Prev APJCP.* 2020;21(11):3365.
49. Rabaan AA, Al-Ahmed SH, Muhammad J, Khan A, Sule AA, Tirupathi R, et al. Role of inflammatory cytokines in COVID-19 patients: a review on molecular mechanisms, immune functions, immunopathology and immunomodulatory drugs to counter cytokine storm. *Vaccines.* 2021;9(5):436.
50. Tse BW, Scott KF, Russell PJ. Paradoxical roles of tumour necrosis factor-alpha in prostate cancer biology. *Prostate cancer.* 2012;2012(1): 128965.
51. Rodríguez-Berriguete G, Sánchez-Espiridión B, Cansino JR, Olmedilla G, Martínez-Onsurbe P, Sanchez-Chapado M, et al. Clinical significance of both tumor and stromal expression of components of the IL-1 and TNF- α signaling pathways in prostate cancer. *Cytokine.* 2013;64(2):555–63.

Publisher's Note Springer Nature remains neutral with regard to jurisdictional claims in published maps and institutional affiliations.